Sensor Set Switching Noise in UWB Indoor Position Tracking

Salil Banerjee*, William Suski and Adam Hoover
Department of Electrical and Computer Engineering
Clemson University, Clemson, SC 29634 USA
Email: salilb@g.clemson.edu, wsuski@clemson.edu, ahoover@clemson.edu

Abstract—**Trilateration calculations are affected by errors in distance measurements from the set of fixed points to the object of interest. When these errors are systemic, each distinct set of fixed points can be said to exhibit a unique set noise. For ultra-wideband (UWB) indoor position tracking, the set of fixed points is a set of sensors measuring the distance to a tracked tag. In this paper we develop a noise model for this sensor set noise, along with a particle filter that uses our set noise model. We test our methods on a real UWB system. Our methods showed an approximately 15% improvement for improving the accuracy of the raw measurements.**

Fig. 1. Changing noise due to sensor set switching.

I. INTRODUCTION

In the early 1980s, the Global Positioning System (GPS) had an accuracy in the range of 100m, useful for ship navigation, aeronautics, and battlefield awareness. Today, GPS accuracy is in the range of 1-2m, providing new applications in vehicle navigation and automated farming. UWB indoor position tracking currently has an accuracy in the range of 30-100cm [1], [2], suitable for applications that require rough room-level precision such as asset tracking [3], indoor navigation and surveillance [4]. Our long-term goal is to improve the accuracy to 1cm or better, expanding potential applications to telepresence, augmented reality, training, entertainment and medical devices [5].

Trilateration-based tracking relies upon measuring the distances from a fixed set of fixed points ("satellites") to an object of interest ("tag"). In this work we consider the noise at the level of a set of satellites used in a single trilateration calculation. This noise changes when the set changes. In a Global Navigation Satellite System (GNSS), set changing happens rarely, because of the scale of the tracking system; one must move a fairly large distance across the Earth to change the set of visible satellites. However, in indoor ultra-wideband (UWB) indoor position tracking, set changing happens frequently. The sets change while moving around a single room, and sometimes even while standing still, depending upon the received signal strengths. In preliminary work our group examined this issue in simulations [6]; in this paper we study it in a real system. We describe a method to model this noise, and a particle filter that uses our noise model. We demonstrate our method on a real UWB indoor position tracking system, providing approximately 15% improvement in tracking accuracy.
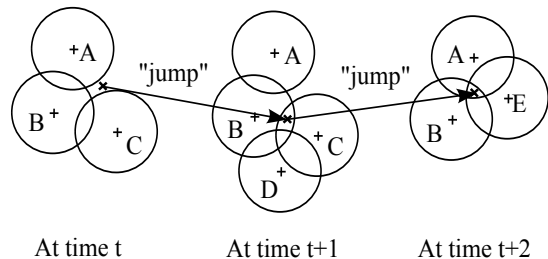
II. METHODS

The problem of fixed point set switching is illustrated in figure 1. The sequence shows three consecutive trilateration calculations that use different sensor sets, each resulting in a different tracked location, even though the object of interest has not moved. At time t, the position of the tag (object of interest) is computed from sensors (fixed points) A, B and C. At time t+1, a new sensor set consisting of A, B, C and D are used to calculate the position of the tag. It can be observed that a change in the sensor set has caused a shift in the calculated position of the tag, due to the changing collective set of noises in the distance measurements. At time t+2, a new set of sensors consisting of A, B and E causes another shift in the calculated position. Hence, switching between sensor sets at each time instant adds a different noise to the measurements corresponding to the noise model of each sensor set. This causes a "jump" in the calculated position of the tag, even when the tag is not moving. A video of such a behavior occurring at our facility using a real UWB position tracking system can be seen at http://youtu.be/B-oCDTBQLd4.

A. UWB positioning system

We used a commercially available UWB based local positioning system developed by Ubisense Inc. (Cambridge, U.K.). We installed eight Series 7000 sensors in the facility at fixed locations. These sensors detect UWB pulses from Ubisense tags [7], which are tracked moving throughout the test area.

Figure 2 shows the positions of the eight sensors distributed across our facility. The company recommends an install where the sensors are placed in a rectangular pattern surrounding the area of interest, with minimum NLOS conditions. However, the promise of UWB indoor position tracking is that it can be
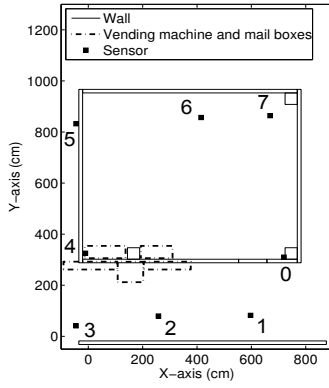
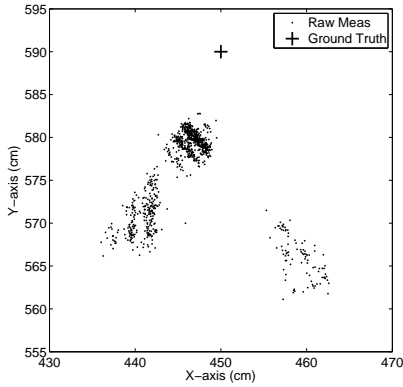Fig. 2. Layout of the facility (0–7 indicate UWB sensor positions).

Fig. 4. Distribution of measurements.

Fig. 3. 1000 measurements collected at a single location (450, 590, 92) cm.

(a) Sensor set 1   (b) Sensor set 2

(a) Sensor set 3   (b) Sensor set 4

Fig. 5. Noise models of four sensor sets at (X,Y,Z) = (450,590,92) cm.

accomplished without direct LOS between the tracked object and fixed sensor points. Our install purposefully introduces some NLOS conditions from the facility in order to explore this challenge. However, it must be noted that NLOS is not the only noise source that contributes to errors in distance measurements for trilateration, and that even with a completely LOS install, we have observed significant sensor set switching noise.

B. Noise model

1) Sensor set: We assume that a tracking measurement is calculated from any subset of the available sensors and each sensor set has a noise model associated with it. We model the noise associated with each sensor set independently. For the sake of simplicity, we assume that the noises are non-zero mean Gaussian, but our methods could be applied with other distributions.

We model the total set of I sensors as $\{1, 2, ..., i_{max}\}$. Let a sensor set s represent any subset of size ≥ 5 sensors drawn from I, denoting a specific sensor subset. We calculate a Gaussian noise model for measurements relative to their actual location for each sensor set s as

$$\mathcal{N}(\mu_x^s, \mu_y^s, \sigma_x^s, \sigma_y^s) \tag{1}$$

The total possible subsets can grow large as the number of sensors I grows. For example, if $\| I \| = 8$, then there are
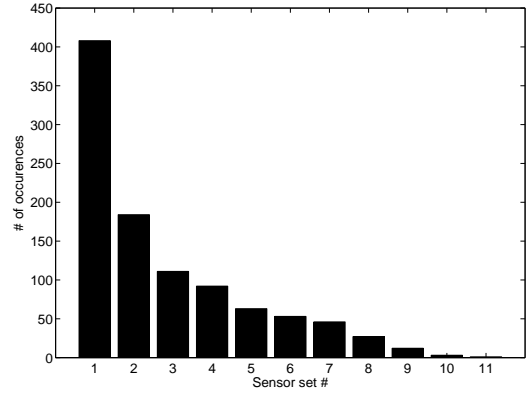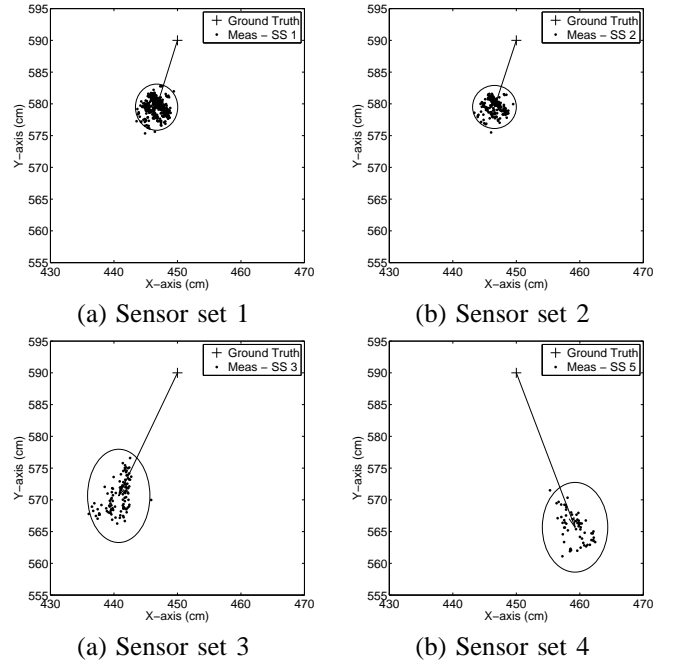
a possible total of $s_{max} = \binom{8}{5} = 56$ sensor sets. However, we assume that a relatively small number of sensor sets dominates the possibilities used for tracking measurements. Figure 3 shows a plot of 1,000 measurements made by our Ubisense system, all at a single ground truth location shown by a '+'. The dots represent the actual measurements received from the system. Figure 4 shows the frequency distribution of the sensor sets for these measurements. The most common 5 sensor sets account for 858 measurements, or 85.8% of the data. These 5 sensor sets are '76540', '75420', '65410', '65420' and '76541', where the numbers indicate the sensor used to provide a measurement. The most commonly occurring sensor set corresponds to the sensors that are most LOS, and therefore generally the most powerful signals. However, it accounts for less than 45% of the total data. The second most commonly occurring sensor set contains a sensor which lies in the hallway and contributes approximately 20% of the

measurements. Similarly, other sensor sets contain at least one sensor which lies in the hallway, providing better angular coverage but more NLOS conditions.

Figure 5 shows the noise models for four sensor sets from the data collected in Figure 3. The noise model for each sensor set is given by $(\mu_x^s, \mu_y^s, \sigma_x^s, \sigma_y^s)$ where (μ_x^s, μ_y^s) corresponds to the average shift of the measurements from the sensor set relative to the ground truth location, and (σ_x^s, σ_y^s) corresponds to the standard deviation of the measurements from their mean. The length of the axes of the ellipses in figure 5 correspond to three standard deviations.

2) Calibration: In order to calculate our noise model, we conduct a calibration step. A tag is placed at a known location, and 1000 measurements are collected. This process is repeated at 6 different locations distributed throughout the facility. The noise parameters $(\mu_x^s, \mu_y^s, \sigma_x^s, \sigma_y^s)$ for each sensor set are calculated at each location, and then weighted-averaged by the number of measurements for each sensor set across the 6 locations. At a single location, if a sensor set has less than 30 measurements then no noise model is calculated at that location. After weighted-averaging, some sensor sets may have no model. We therefore also calculate a facility-wide noise model that is used by default for measurements taken from a non-modeled sensor set. The facility-wide noise model is taken as the average of all measurements taken during the calibration step.

C. Set noise particle filter

We assume a 2D linear constant velocity model in our experiments. Let the state of the system $\mathbf{X}$ be defined as

$$\mathbf{X} = \begin{bmatrix} x_t \\ \dot{x}_t \\ y_t \\ \dot{y}_t \end{bmatrix} \qquad (2)$$

where, x_t, y_t are the positions along the x and y axes at time t and $\dot{x}_t, \dot{y}_t$ are the velocities.

The system transition equations $\boldsymbol{f}$ are

$$\boldsymbol{f} = \begin{bmatrix} x_{t+1} = x_t + T\dot{x}_t \\ \dot{x}_{t+1} = \dot{x}_t + \mathcal{N}(0, \sigma_d) \\ y_{t+1} = y_t + T\dot{y}_t \\ \dot{y}_{t+1} = \dot{y}_t + \mathcal{N}(0, \sigma_d) \end{bmatrix} \qquad (3)$$

where $\mathcal{N}(0, \sigma_d)$ is a continuous zero-mean Gaussian random variable. The dynamic noise $\mathbf{U_t}$ denotes the dynamic noise during a state transition:

$$\mathbf{U}_t = \begin{bmatrix} 0 \\ \mathcal{N}(0, \sigma_d) \\ 0 \\ \mathcal{N}(0, \sigma_d) \end{bmatrix} \qquad (4)$$

The dynamic noise models a potential change in velocity during each time step.

At each time t, the set of observed values $\mathbf{Z}$ is

$$\mathbf{Z} = \begin{bmatrix} \tilde{s}_t \\ \tilde{x}_t \\ \tilde{y}_t \end{bmatrix} \qquad (5)$$

where $\tilde{s}_t$ is the sensor set used to measure $\tilde{x}_t, \tilde{y}_t$. The observation equations $\boldsymbol{g}$ are

$$\boldsymbol{g} = \begin{bmatrix} \tilde{s}_t \leftarrow \{1, 2, ..., s_{max}\} \\ \tilde{x}_t = x_t + \mathcal{N}(\mu_x^{\tilde{s}_t}, \sigma_x^{\tilde{s}_t}) \\ \tilde{y}_t = y_t + \mathcal{N}(\mu_y^{\tilde{s}_t}, \sigma_y^{\tilde{s}_t}) \end{bmatrix} \qquad (6)$$

where it is assumed that a random non-zero mean Gaussian noise associated with sensor set $\tilde{s}_t$ has been added to the actual position to produce the measurement.

Particle filtering is a sequential Monte Carlo methodology where the posterior density function is recursively approximated using a set of random samples and weights, from which estimates are computed [8], [9]. The number of samples K depends on how accurately we want to model the posterior density; in this work we use $K = 1000$.

In our experiments, we initialize all particles to have equal weight and the same initial state:

$$\chi = \left\{\mathbf{X}^k, w^k\right\}_{k=1}^K = \left\{ \begin{bmatrix} x_0 \\ 0 \\ y_0 \\ 0 \end{bmatrix}, \frac{1}{K} \right\} \qquad (7)$$

where x_0 and y_0 are the known starting position of the tag along the x and y axes with zero initial velocities.

An observation $\mathbf{Z}_t$ is taken. We use sequential importance sampling using the prior importance function [9], so that the weights for the particles are updated according to

$$w_t^k = w_{t-1}^k p(\mathbf{Z}_t | \mathbf{X}_t^k) \qquad (8)$$

The weight update step given by

$$p(\mathbf{Z}_t | \mathbf{X}_t^k) = \exp - \left(\frac{((x_t^k - \mu_x^{\tilde{s}_t}) - \tilde{x}_t)^2}{2(\sigma_x^{\tilde{s}_t})^2} + \frac{((y_t^k - \mu_y^{\tilde{s}_t}) - \tilde{y}_t)^2}{2(\sigma_y^{\tilde{s}_t})^2} \right) \qquad (9)$$

where $(x_t^k - \mu_x^{\tilde{s}_t})$ and $(y_t^k - \mu_y^{\tilde{s}_t})$ gives the most probable measurement of each particle. Equation 9 calculates the likelihood of obtaining the actual observed measurement relative to the most probable state of the particle, according to the measurement noise distribution associated with the sensor set used to take the measurement.

Collectively, the discrete values of the particles represent a continuous probability distribution function (pdf) of the state at a particular time. After updating the weights, they must be normalized:

$$\left\{ w_t^k = \frac{w_t^k}{\sum_{i=1}^K w_t^i} \right\}_{k=1}^K \qquad (10)$$

We then calculate the expected value of the set of particles as output:

$$E[\chi] = \sum_{k=1}^K \mathbf{X}^k w^k \qquad (11)$$

Particle filtering is well-known to suffer from a degradation over time where particle weights tend towards zero. In order
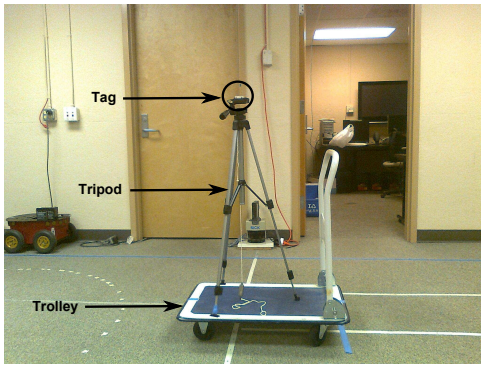
Fig. 6. Setup used to collect recordings.

Fig. 7. Test tracks in the facility.

to counter this effect, we follow the general strategy of resampling when a sizable percentage of particles reaches negligible weight. Following methods outlined in [10], we calculate the coefficient of variation (CV) as

$$CV = \frac{VAR(w^k)}{(E[w^k])^2} = \frac{1}{K}\sum_{k=1}^{K}(Kw^k - 1)^2 \qquad (12)$$

The effective sample size is calculated as $ESS = \frac{K}{1+CV}$. This factor indicates if there are sufficient particles having appreciable weight and whether resampling is necessary. If $ESS < 0.5$, we resample using the select with replacement algorithm [10].

D. Data collection

Figure 6 shows the apparatus used to record experimental data for testing. A tag was placed on a tripod resting on a trolley. The tripod was adjusted so that it would match up to the same height (92 cm) used to collect calibration data. The trolley was then pulled manually along a track laid on the ground at different speeds. For each recording, the apparatus was pulled back and forth seven times along a 250 cm straight line. The total distance covered in each recording is 1750 cm.

Figure 7 shows the location of the track in the test area. For each recording along the track, the Ubisense system provides raw measurements of the tag along the X and Y axes, and the sensors used to calculate each measurement. We turned off the simple averaging filters provided by the Ubisense system and collected the raw measurements.

Five recordings were collected along the track at different speeds. The speed was varied from ≈11 cm/s (extremely slow motion) to ≈120 cm/s (walk speed) [11]. Table I lists the recording number and the approximate speed of the recording. The speeds were chosen to test the viability of our method for a range of motion dynamics resembling a slow moving robot to the walking of a person.

E. Ground Truth

We use a least squares approach to calculate the ground truth data. Since we assume that the tag is moving with a constant velocity, we can associate each measurement with a ground truth location. The velocity is calculated by dividing
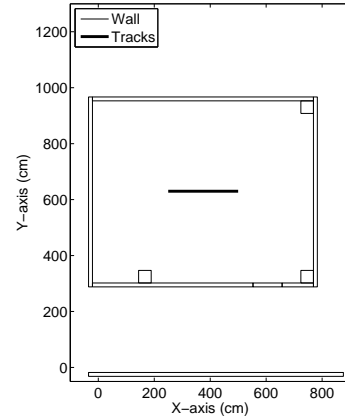
TABLE I
RANGE OF MOTIONS

Recording #	Total Measurements	Speed (cm/s)	Raw Error (cm)
1	1521	11	18
2	467	35	19
3	250	65	21
4	164	100	23
5	135	120	22

the total ground truth distance covered by the total time taken when the tag is in motion. Now, multiplying the velocity by the time at which the measurement was received gives us the corresponding ground truth position of the tag at that time instant.

III. EXPERIMENTAL RESULTS

The output for the particle filter is to some degree controlled by the value chosen for σ_d (see equation 4), the dynamic noise in the motion model. This value represents the amount of expected change in velocity at each time step. The lower this value, the more the filter weights the output towards the system equations, in essence providing more smoothing. The higher this value, the more the filter weights the output towards the measurements, allowing a quicker reaction to actual dynamics at the cost of less smoothing.

Figure 8 shows the raw measurements and set noise particle filter output for this recording at $\sigma_d = 6.0$ cm/s. For clarity, only a subset of the data is shown, and only the X-coordinates are shown (the motion is along a straight line of constant Y). Because the optimal value of σ_d was chosen for this figure, it can be seen that both filters provide a fairly good output that is better than the raw measurements. However, it can also be seen that the set noise particle filter output is more accurate, particularly in the range of measurements from 80 to 120.

Figure 9 shows the average error curves for all five recordings. The error curves are the average Euclidean distance errors of the recordings over 100 trials (repeated runs of each filter at each value of σ_d); this is necessary because the particle filter is a Monte Carlo approach and a single trial of limited
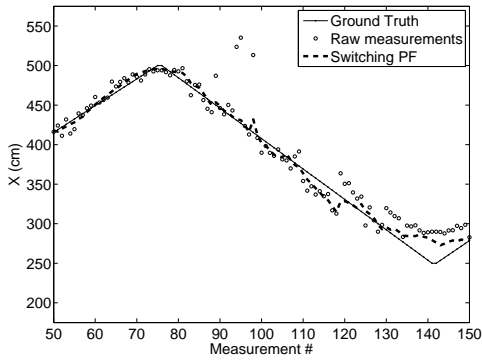
Fig. 8. Recording 2 at σ_d = 6.0 cm/s (partial output along X-axis).
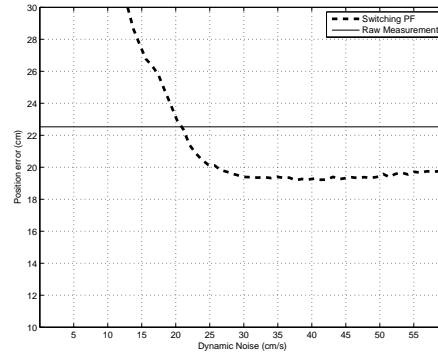

Fig. 9. Average error curve for all recordings.

length does not necessarily provide a typical representative output. The average accuracy of the raw measurements is approximately 23 cm. The range of $\sigma_d = 30$ to 50 cm/s shows that the set noise particle filter improved the accuracy of the raw measurements by approximately 5 cm on average. Thus, our set noise particle filter shows an approximately 15% improvement over raw measurements.

IV. CONCLUSION AND FUTURE WORK

The contribution of this paper is that we have identified a new noise source due to the switching of fixed point sets for trilateration. While this noise is theoretically present in all trilateration-based systems, it is not readily apparent in large-scale systems like the GPS, but it can cause noticeable jump-like behavior in indoor UWB position tracking. We have developed a mathematical model and particle filter that accounts for this noise. We tested our methods on a real UWB indoor position tracking system. Our set noise particle filter showed an approximately 15% improvement in improving the accuracy of the raw measurements.

Our experiments have been conducted in a semi-controlled but real world setting. Even with the semi-controlled setting, we have achieved modest improvement in the tracking accuracy over a range of dynamics. However, we have observed that noise due to NLOS, multipath and timing errors tend to be more significant than noise caused by sensor set switching. Hence, research studying the impact of these noise sources in isolation have been able to achieve sub-decimeter [12], [13] and sometimes even sub-centimeter accuracies [14], [15], while we have been able to observe only a modest improvement. In practice, we believe that our set noise filter should be combined with filters specifically designed for other noise sources. This is a subject for future work.

ACKNOWLEDGMENT

REFERENCES

[1] M. Navarro and M. Najar, "TOA and DOA Estimation for Positioning and Tracking in IR-UWB," in *IEEE International Conference on Ultra-Wideband (ICUWB)*, sept. 2007, pp. 574–579.

[2] M. Kuhn, C. Zhang, B. Merkl, D. Yang, Y. Wang, M. Mahfouz, and A. Fathy, "High accuracy UWB localization in dense indoor environments," in *IEEE International Conference on Ultra-Wideband (ICUWB)*, vol. 2, sept. 2008, pp. 129–132.

[3] R. Mautz, "Overview of Current Indoor Positioning Systems," in *Geodesy and Cartography*, vol. 34, no. 2, 2009, pp. 66–70.

[4] K. W. Kolodziej and J. Hjelm, *Local Positioning Systems: LBS Applications and Services*. CRC Press, 2006.

[5] A. Ghildiyal, K. Amara, R. Molin, B. Godara, A. Amara, and R. Shevgaonkar, "UWB for in-body medical implants: A viable option," in *IEEE International Conference on Ultra-Wideband (ICUWB)*, vol. 2, sept. 2010, pp. 1–4.

[6] D. Ganjali, "Filtering Noise Caused by Sensor Selection for an Ultra-Wideband position tracking system," Master's thesis, Clemson University, December 2009.

[7] "Series 7000 Compact Tag," http://www.ubisense.net/en/resources/factsheets/series-7000-compact-tag.html.

[8] M. Arulampalam, S. Maskell, N. Gordon, and T. Clapp, "A tutorial on particle filters for online nonlinear/non-Gaussian Bayesian tracking," *IEEE Transactions on Signal Processing*, vol. 50, no. 2, pp. 174 –188, Feb. 2002.

[9] P. Djuric, J. Kotecha, J. Zhang, Y. Huang, T. Ghirmai, M. Bugallo, and J. Miguez, "Particle filtering," *IEEE Signal Processing Magazine*, vol. 20, no. 5, pp. 19 – 38, Sep. 2003.

[10] I. M. Rekleitis, "A particle filter tutorial for mobile robot localization, Technical Report TR-CIM-04-02," Centre for Intelligent Machines, McGill University, Tech. Rep., 2004.

[11] R. Knoblauch, M. Pietrucha, and M. Nitzburg, "Field Studies of Pedestrian Walking Speed and Start-Up Time," *Transportation Research Record*, vol. 1538, no. 1, pp. 27–38, 1996.

[12] Z. Low, J. Cheong, C. Law, W. Ng, and Y. Lee, "Pulse detection algorithm for line-of-sight (los) uwb ranging applications," *IEEE Antennas and Wireless Propagation Letters*, vol. 4, pp. 63 – 67, 2005.

[13] G. MacGougan, K. O'Keefe, and R. Klukas, "Tightly-coupled GPS/UWB Integration," *The Journal of Navigation*, vol. 63, no. 01, pp. 1–22, 2010.

[14] M. Mahfouz, C. Zhang, B. Merkl, M. Kuhn, and A. Fathy, "Investigation of High-Accuracy Indoor 3-D Positioning Using UWB Technology," *IEEE Transactions on Microwave Theory and Techniques*, vol. 56, no. 6, pp. 1316 –1330, June 2008.

[15] R. Zetik, J. Sachs, and R. Thoma, "UWB localization - active and passive approach [ultra wideband radar]," in *Proceedings of the 21st IEEE Instrumentation and Measurement Technology Conference*, vol. 2, May 2004, pp. 1005 – 1009.